J. Water Environ. Nanotechnol., 2(4): 290-301 Autumn 2017

ORIGINAL RESEARCH PAPER

Photocatalytic Treatment of Synthetic Wastewater Containing 2,4 dichlorophenol by Ternary MWCNTs /Co-TiO_2 Nanocomposite Under Visible Light

Shahryar Nazarpour Laghani [1], Azadeh Ebrahimian Pirbazari [1,2,*]

[1] Caspian Faculty of Engineering, College of Engineering, University of Tehran, Rezvanshahr, Iran.
[2] Fouman Faculty of Engineering, College of Engineering, University of Tehran ,Fouman, Iran.

Received: 2017-03-10 Accepted: 2017-10-09 Published: 2017-10-15

ABSTRACT
In this work, multi-walled carbon nanotubes (MWCNTs)/Co-TiO_2 nanocomposites were synthesized and investigated for photocatalytic degradation of 2,4-dichlorophenol (2,4-DCP) under visible light. Characterization of photocatalysts was done by means of XRD, FT-IR and SEM/EDX techniques. Obtained results showed cobalt doping can inhibit phase transformation from anatase to rutile and eliminate the recombination of electron-hole pairs. The presence of MWCNTs can both increase the photoactivity and change surface properties to achieve sensitivity to visible light. The optimum mass ratio of MWCNTs and cobalt (Co) dopant in TiO_2 was the prominent factor to harvest MWCNTs/Co-TiO_2 photocatalyst. The sample containing 3.13 wt% cobalt exhibited the highest activity under visible light for 2,4-DCP degradation, which was completed within 180 min using a 0.1 g/L dose of this photocatalyst in a 40 mg/L solution of the 2,4-DCP. The reactions follow the first-order kinetics. The reaction intermediates were identified by GC–MS technique. GC–MS analysis showed the major intermediates of 2,4-DCP degradation are simple acids like oxalic acid, acetic acid, etc. as the final products.

Keywords: *Carbon Nanotubes, Cobalt, 2,4-dichlorophenol, Degradation.*

How to cite this article
Nazarpour Laghani S, Ebrahimian Pirbazari A. Photocatalytic Treatment of Synthetic Wastewater Containing 2,4 dichlorophenol by Ternary MWCNTs /Co-TiO_2 Nanocomposite Under Visible Light. J. Water Environ. Nanotechnol., 2017; 2(4): 290-301. DOI: 10.22090/jwent.2017.04.006

INTRODUCTION

With the rapid development of industrialization, certain hazardous effects on the environment and human survival have emerged beside its benefit. Effluents from the use of pesticides, the textile, petrochemical, dyeing, plastic, and paper industries are highly toxic, carcinogenic and recalcitrant [1,2], and yet not readily degradable. Chlorophenols are toxic chemicals which are used in many industrial applications such as petrochemicals, pesticide, dye intermediates and paint [3]. Especially, 2,4-dichlorophenol (2,4-DCP) is an important chemical precursor for the manufacture of a widely used herbicide, 2,4-dichlorophenoxy acetic acid (2,4-D) [4]. However, 2,4-DCP may cause some pathological symptoms and changes to human endocrine systems. Their mode of exposure is through the skin and gastrointestinal tract. In recent years, concerns have been raised because of chlorophenols persistence and bioaccumulation both in animals and in humans [5-7].Therefore, it is important to find innovative and effective ways to minimize the harm of chlorophenols in the environment. Heterogeneous semiconductor photocatalysts have received significant attention owing to their potential application in a wide range

* Corresponding Author Email: *aebrahimian@ut.ac.ir*

of photoinduced reactions, notably photocatalytic hydrogen production, removal of organic contaminants and air pollutants, and electricity production using solar cells [8–11]. TiO_2 mediated photocatalytic degradation is a successful and convenient alternative to the conventional methods for the treatment of wastewater containing organic pollutants. TiO_2 has the advantage of good chemical stability, the absence of toxicity and relatively low cost, but a serious disadvantage is its wide band gap (Eg = 3.2 eV) that requires that UV radiation is used to trigger this attractive photocatalyst, which would greatly hinder the commercialization of TiO_2 photocatalysis. Photocatalytic degradation of organic contaminants using abundant natural solar radiation can be highly economical compared with the processes using artificial UV radiation, which require substantial electrical power input. In regard to this, various attempts have been made to extend the spectral response of TiO_2 into the visible region of the solar spectrum and enhance its photocatalytic activity [12]. Lots of attempts were tried to improve the photocatalytic performance of TiO_2 and doping with transition metal ions, such as silver, nickel, and iron was found to be a useful method [13-18]. Among all the available transition metals, cobalt was proved to be one of the most effective dopants to enhance the light response and photoactivity of TiO_2. Ebrahimian and *et al* [19] prepared cobalt doped TiO_2 nanoparticles which shows a wide absorption range extended into the visible region. Iwasaki [20] synthesized cobalt doped TiO_2 and found that the introduction of Co^{2+} could apparently shift the light absorption edge of anatase TiO_2 to the visible region and enhance photoactivity under both UV and visible light irradiation. Also, researchers found that the addition of co-sorbent carbon materials can enhance the photocatalytic efficiency of TiO_2 [21-23]. As a new member of the carbon family, carbon nanotubes (CNTs) with one-dimensional and hollow structure have received considerable interest since their discovery [24] due to their outstanding structural characters, e.g., mechanical strength [25], excellent thermal conductivity, unique electronic properties [26] and thermal stability [27]. CNTs can be used as a promising material for environmental cleaning. The collection process for MWCNTs with TiO_2 in new composite depends on many causes: one of them suggests that carbon nanotubes behave as a semiconductor supports because of their combination of physiochemical properties which include excellent conductance, high abilities for adsorption [28]. A similar literature has shown that the activities of TiO_2 increased due to abilities of MWCNTs to decrease TiO_2 crystalline grain and particle sizes [29], or increased in the activity of the particles because the direct interaction between MWCNTs and TiO_2 reduces the recombination of electron and hole (h^+/e^-) [30]. Generally, It is believed that the change on activities can be related to the TiO_2–CNTs bonding which can be formed through some physic/chemical interactions such as Vander Walls interaction. The above finding stimulated the advance improvement of an efficient photocatalyst in visible light region. To the best of our knowledge, MWCNTs /Co-TiO_2 nanocomposites prepared using modified sol-gel process have not yet been reported. In the present work, these nanocomposites were prepared using titanium isopropoxide (TIP) as titanium precursor. The performance of the resultant photocatalysts was evaluated by photocatalytic treatment of synthetic wastewater containing 2,4 dichlorophenol (2,4-DCP) under visible light. The textural properties of the resulting photocatalysts were investigated using XRD, FTIR and SEM/EDX. The reaction intermediates were identified by gas chromatography-mass spectrometry (GC–MS) technique.

EXPERIMENTAL

Materials and reagents

Cobalt (II) chloride hexahydrate ($CoCl_2.6H_2O$) was supplied by (Merck, No.102539). Titanium isopropoxide (TIP), (Merck No. 8.21895), ethanol (Merck No. 818760), deionized water and multi-walled carbon nanotubes functionalized by carboxylic groups (MWCNTs) were provided by Neutrino Corporation (Iran), (The average diameter of the MWCNTs was 10-20 nm, and the length was 0.5-2μm), were used for photocatalyst synthesis. High-purity 2,4-DCP, 98%, (Merck No. 803774) was used as a probe molecule for photocatalytic tests.

Preparation of MWCNTs/Co-TiO_2 nanocomposite

MWCNTs/Co-TiO_2 nanocomposite was prepared by a modified sol-gel method. An appropriate amount of $CoCl_2.6H_2O$ (Table 1), 10 mL TIP and 30 mL ethanol were stirred for 2 h (Solution A). Then, solution B, 20 mL ethanol, 5 mL deionized water and 2 mL hydrochloric acid and an amount of MWCNTs (Table 1) was

Table 1: Nomenclatures of the prepared samples

Samples	Materials	Nomenclatures
TiO_2	TiO_2	TiO_2
MWCNTs	MWCNTs	MWCNTs
MWCNTs/TiO_2	0.55* g MWCNTs + TiO_2	MWCNTs/TiO_2
Co-TiO_2	0.48 g $CoCl_2.6H_2O$ + TiO_2	Co-TiO_2
MWCNTs/ Co-TiO_2	0.03 g MWCNTs + 0.48 g $CoCl_2.6H_2O$ + TiO_2	MWCNTs/ Co-TiO_2 (3.03)**
MWCNTs/ Co-TiO_2	0.04 g MWCNTs + 0.48 g $CoCl_2.6H_2O$ + TiO_2	MWCNTs/ Co-TiO_2 (3.13)
MWCNTs/ Co-TiO_2	0.05 g MWCNTs + 0.48 g $CoCl_2.6H_2O$ + TiO_2	MWCNTs/ Co-TiO_2 (3.52)
MWCNTs/ Co-TiO_2	0.10 g MWCNTs + 0.48 g $CoCl_2.6H_2O$ + TiO_2	MWCNTs/ Co-TiO_2 (4.14)

*The average amount of MWCNTs that used for synthesis of MWCNTs/ Co-TiO_2 samples.

**The number in parenthesis is the weight percent of cobalt in the final solid that obtained by EDX analysis.

added into the Solution A and stirred for 12 h at room temperature. The sol was formed after 12 h of stirring followed by aging at room temperature for 24 h and evaporated at 80 °C for 8 h. Finally, the dried powder was calcined at 450 °C under air for 2 h to get an MWCNTs/Co-TiO_2 sample. For comparison, four MWCNTs/Co-TiO_2 samples with different amounts of MWCNTs, pure TiO_2, Co-TiO_2 and MWCNTs/TiO_2 samples were synthesized by the same route. From now on, the prepared samples will be shown according to Table 1.

Characterization

Fourier transforms infrared (FTIR) analysis was applied to determine the surface, functional groups, using FTIR spectroscopy (FTIR-2000, Bruker), where the spectra were recorded from 4000 to 400 cm^{-1}. The XRD patterns were recorded on a Siemens, D5000 (Germany). X-ray diffractometer using Cu K_α radiation as the X-ray source. The diffractograms were recorded in the 2θ range of 20-80°. The morphology of the prepared samples was characterized using scanning electron microscope (SEM) (Vegall-Tescan Company) equipped with an energy dispersive X-ray (EDX).

Photocatalytic degradation of 2,4-DCP

In a typical run, the suspension containing 10 mg photocatalyst and 100 mL aqueous solution of 2,4-DCP (40 mg/L) was stirred first in the dark for 10 min to establish adsorption/desorption equilibrium. Irradiation experiments were carried out in a self-built reactor. A visible (Halogen, ECO OSRAM, 500W) lamp was used as irradiation source (its emitting wavelength ranges from 350 nm to 800 nm with the predominant peak at 575 nm).At certain intervals, small aliquots (2 mL) were withdrawn and filtered to remove the photocatalyst particles. These aliquots were used for monitoring the degradation progress, with Rayleigh UV-2601 UV/VIS spectrophotometer (λ_{max}= 227nm).

Statistical analysis

All experiments were performed in triplicate and the average values were presented. The data were analyzed by one-way analysis of variance (ANOVA) using SPSS 11.5 for Windows. The data were considered statistically different from control at $P < 0.05$.

Identification of degradation intermediates

The photocatalytic reaction intermediates were identified by GC–MS in an Agilent 190915-433 instrument equipped with an HP-5MS capillary column (30 m × 0.25 mm). The column temperature was programmed at 50 °C for 2 min, and from 50 to 250 °C at a rate of 10 °C min^{-1}. The sample used for GC–MS analysis was prepared according to the following procedure: The obtained degradation product was acidified to pH 1 and subsequently extracted with dichloromethane. After dichloromethane was evaporated to dryness under vacuum, 10 mL methanol was added to dissolve the residue. Then, 1 mL concentrated sulfuric acid was added and the combined solution was refluxed for about 3 h. The solution was further extracted with dichloromethane followed by concentrating to about 1 mL under reduced pressure. The released chloride ions originating from the degradation of 2,4-DCP were identified and determined by the $AgNO_3$ method.

RESULT AND DISCUSSION

X-ray diffraction analysis

Fig. 1a shows the XRD pattern of the prepared TiO_2. The diffractions found at 2θ= 27.4°, 36.1°, and 41.2° belonged to the rutile crystalline phase of TiO_2 [31] and the diffractions at 2θ= 25.28°, 37.80°, 48.18°, and 54.09 are the main diffractions for the anatase crystalline phase of TiO_2 (JCPDS 21-1272). The XRD pattern revealed the prepared TiO_2 containing predominant anatase crystalline phase and a few of rutile crystalline phase. The

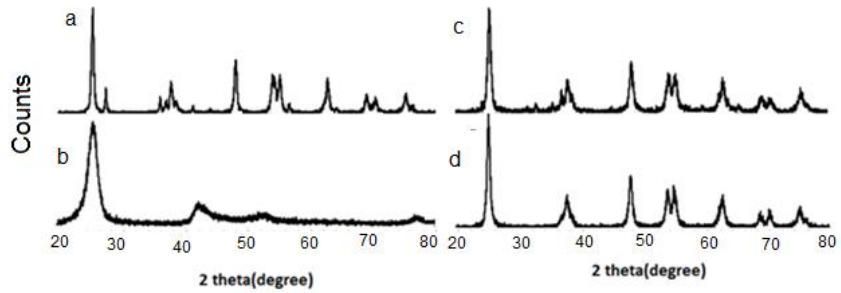

Fig. 1: The XRD patterns of a) TiO_2, b) MWCNTs, c) MWCNTs/TiO_2 and d) Co-TiO_2

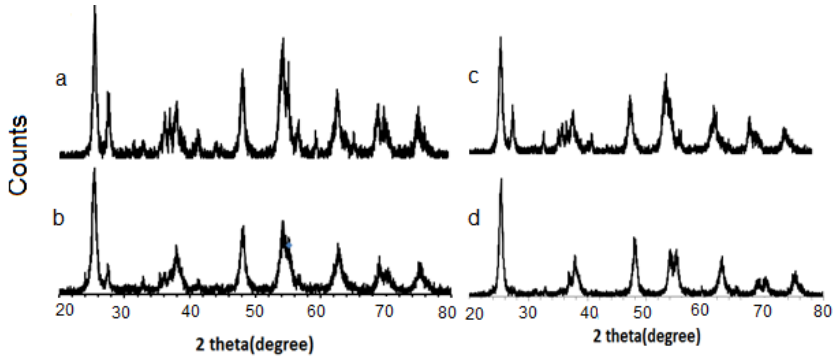

Fig. 2: The XRD patterns of a) MWCNTs/ Co-TiO_2 (3.03), b) MWCNTs/ Co-TiO_2 (3.13), c) MWCNTs/ Co-TiO_2 (3.52) and d) MWCNTs/ Co-TiO_2 (4.14)

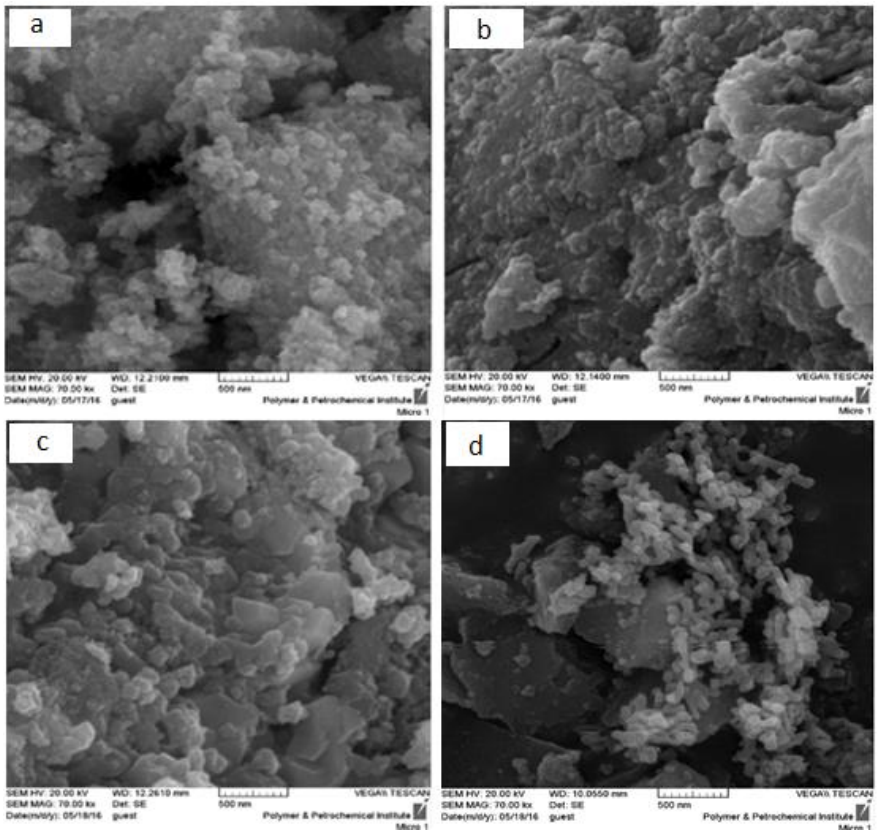

Fig. 3: SEM micrographs of a) MWCNTs/ Co-TiO_2 (3.03), b) MWCNTs/ Co-TiO_2 (3.13), c) MWCNTs/ Co-TiO_2 (3.52) and d) MWCNTs/ Co-TiO_2 (4.14)

Table 2: Phase and average crystal size of the prepared samples

Sample	Phase	Average crystal size (nm)
TiO_2	Anatase-Rutile	18.32
MWCNTs/TiO_2	Anatase	15.00
Co-TiO_2	Anatase	15.49
MWCNTs/ Co-TiO_2 (3.03)	Anatase-Rutile	12.32
MWCNTs/ Co-TiO_2 (3.13)	Anatase-Rutile	10.11
MWCNTs/ Co-TiO_2 (3.52)	Anatase-Rutile	11.19
MWCNTs/ Co-TiO_2 (4.14)	Anatase	11.52

Table 3: Elemental chemical analysis of the MWCNTs/Co-TiO_2 samples

Sample	C wt%	Ti wt%	O wt%	Co wt%
MWCNTs/Co-TiO_2(3.03)	9.01	38.27	49.68	3.03
MWCNTs/Co-TiO_2(3.13)	7.80	37.87	51.19	3.13
MWCNTs/Co-TiO_2(3.52)	7.01	44.13	45.35	3.52
MWCNTs/Co-TiO_2(4.14)	8.46	42.92	44.48	4.14

XRD pattern of MWCNTs (Fig. 1b) shows a broad crystalline diffraction around 2θ=25.5°, which represents the characteristic diffraction of MWCNTs [32]. In XRD pattern of MWCNTs/ TiO_2 (Fig. 1c), we didn't observe the strong and main diffraction of MWCNTs at 2θ=25.5°, which was overlapped with the main diffraction of anatase TiO_2 at 2θ=25.3° and the relatively large difference between the mass percent of MWCNTs and TiO_2 and low crystallinity of MWCNTs could be the reasons for the MWCNTs diffraction not to be detectable [33]. Also, the XRD pattern of Co-TiO_2 sample (Fig. 1d) didn't show any cobalt phase indicating that cobalt ions uniformly dispersed among the anatase crystallites and showed only pure anatase phase for TiO_2 [34-37]. The XRD patterns of the ternary MWCNTs/Co-TiO_2 nanocomposites (Fig. 2) revealed the main diffractions of anatase and rutile crystalline phase for TiO_2. Also, the XRD patterns (Fig. 2), showed, increasing of cobalt doping inhibited the phase transformation from anatase to rutile in the ternary MWCNTs/Co-TiO_2 nanocomposites [38] and we observed pure anatase crystalline phase for the sample MWCNTs/Co-TiO_2 (4.14) (containing the highest cobalt doping in our synthesized samples) (Fig. 2d).

The diffraction patterns of the prepared samples show considerable line width, indicating the samples containing small crystal. The average crystal size of each sample is calculated from the full width at half maximum (FWHM) of the (101) diffraction peak using Scherrer's equation [39].

$$D = \frac{K\lambda}{\beta \cos\theta} \quad (1)$$

Where D is the average crystal size of the sample, λ the X-ray wavelength (1.54056 Å), β the full width at half maximum (FWHM) of the diffraction peak (radian), K is a coefficient (0.89) and θ is the diffraction angle at the peak maximum. All the prepared samples are in nano-size range (Table. 2), from 10.11 to 18.32 nm, and all the samples showed smaller crystal size compared to pure TiO_2. In the case of ternary MWCNTs/ Co-TiO_2 nanocomposites, it can be concluded that the addition of cobalt to titania hinders the growth of TiO_2 nanoparticles. This may be due to the formation of Co–O bond on the surface of the doped TiO_2, which restricted the crystallite growth of TiO_2 [40].

SEM/EDX analysis

SEM images of the ternary MWCNTs/Co-TiO_2 nanocomposites are shown in Fig. 3. Some aggregation can be observed that probably happened during the synthesis process. The high viscosity of the sol might be one of the reasons to induce this phenomenon [41]. The EDX patterns of the ternary MWCNTs/Co-TiO_2 nanocomposites in Fig. 4 show two peaks around 0.2 and 4.5 keV. The intense peak is assigned to the bulk TiO_2 and the less intense one to the surface TiO_2. The peaks of cobalt are distinct in Fig. 4 at 0.6, 6.9 and 7.5 keV. The less intense peak is assigned to cobalt in the TiO_2 lattice [42, 43]. These results confirmed the existence of cobalt atoms in the ternary MWCNTs/ Co-TiO_2 nanocomposites but the XRD patterns do not show any diffractions related to cobalt. Therefore, it may be concluded that cobalt ions are uniformly dispersed among the TiO_2 lattice during the synthesis process. EDX results are given in Table 3. Fig. 5 shows elemental mapping images of the ternary MWCNTs/Co-TiO_2 nanocomposites. From the elemental mapping mode, highly and

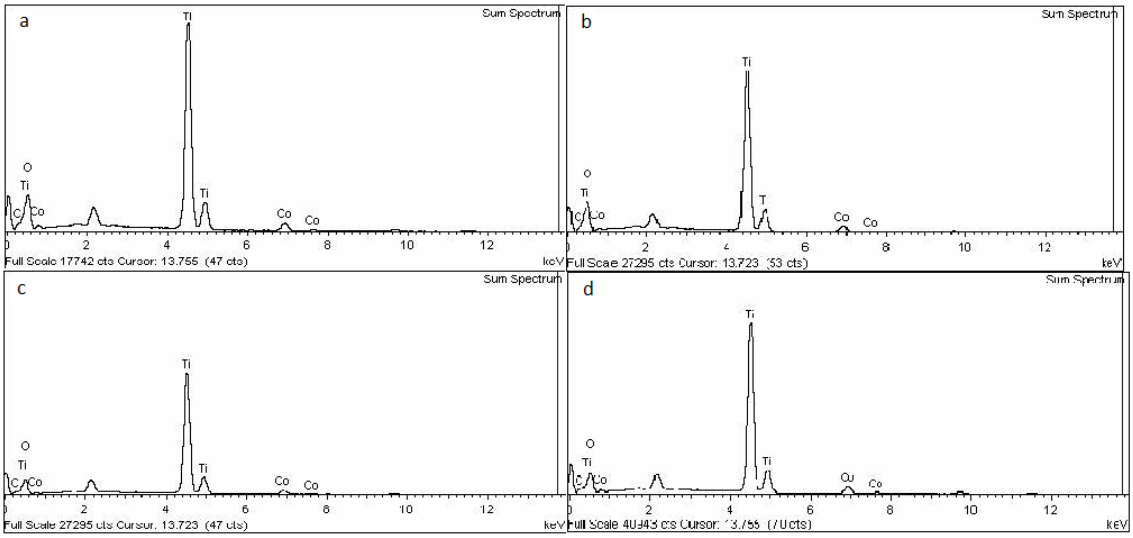

Fig. 4: EDX patterns of a) MWCNTs/ Co-TiO_2 (3.03), b) MWCNTs/ Co-TiO_2 (3.13), c) MWCNTs/ Co-TiO_2 (3.52) and d) MWCNTs/ Co-TiO_2 (4.14).

uniformly dispersion of cobalt was observed in the TiO_2 lattice especially for the sample MWCNTs/ Co-TiO_2 (3.13). This implies a good interaction between cobalt and TiO_2 in the preparation process using the sol-gel method.

FTIR analysis

The FTIR spectra of the ternary MWCNTs/ Co-TiO_2 nanocomposites are shown in Fig. 6. The vibrations observed at ~3400, 2930 and 2850 cm^{-1} are attributed to the Ti – OH bond [44]. The spectra show the relatively strong band at ~ 1630 cm^{-1} observed for all the samples which are due to the OH bending vibration of chemisorbed and/or physisorbed water molecule on the surface of the catalysts. The strong vibration in the range of 700-500 cm^{-1} is attributed to stretching vibrations of Ti –O–Ti bond [44]. The weak peak at about 514 cm^{-1} assigned to stretching vibrations of Co–O emerged a little [45], the Co–O vibration is not strong because of the broad spectrum of TiO_2 and a small amount of Co dopant. FT-IR results reminded the formation of a small part of Co–O bond. It was probably the existence of Co–O bond that hindered the recombination of generated photo holes and photoelectrons [40]. FTIR results showed the ternary MWCNTs/Co-TiO_2 nanocomposites contain MWCNTs, cobalt, and TiO_2.

Photocatalytic degradation of 2,4-DCP

The photocatalytic degradation efficiency of 2,4-DCP using the prepared samples under visible light showed in Fig.7 and Table 4. Among the ternary nanocomposites, the photocatalytic activity of the MWCNTs/Co-TiO_2 (3.13) sample was the highest and 82% degradation of 2,4-DCP obtained after 180min irradiation under visible light. We obtained the degradation percent of 2,4-DCP in the presence of pure TiO_2, MWCNTs/TiO_2 and Co-TiO_2 samples, 44%, 71% and 67%, respectively during 180min under visible light. The degradation percent of 2,4-DCP in the presence of the ternary MWCNTs/Co-TiO_2 nanocomposites is higher than pure TiO_2, it can be noticed that the introduction of MWCNTs and cobalt obviously caused a synergetic effect on 2,4-DCP degradation and led to a higher photocatalytic activity (Table 4). The higher photocatalytic activity of MWCNTs and Co co-modified TiO_2 in the ternary nanocomposites may be explained as firstly, an appropriate amount of the doped Co in TiO_2 could effectively capture the photo-induced electrons and holes, which inhibited the combination of photoinduced carriers and improved the photocatalytic activity. Secondly, MWCNTs/Co-TiO_2 samples had more surface hydroxyl groups than the pure TiO_2 sample which would be beneficial for the adsorption of 2,4-DCP.

Table 4: Degradation percent of 2,4-DCP under visible light after 180 min.

Sample	%Removal
TiO_2	44.01
MWCNTs/TiO_2	70.81
Co-TiO_2	67.00
MWCNTs/ Co-TiO_2 (3.03)	65.67
MWCNTs/ Co-TiO_2 (3.13)	82.03
MWCNTs/ Co-TiO_2 (3.52)	69.80
MWCNTs/ Co-TiO_2 (4.14)	60.91

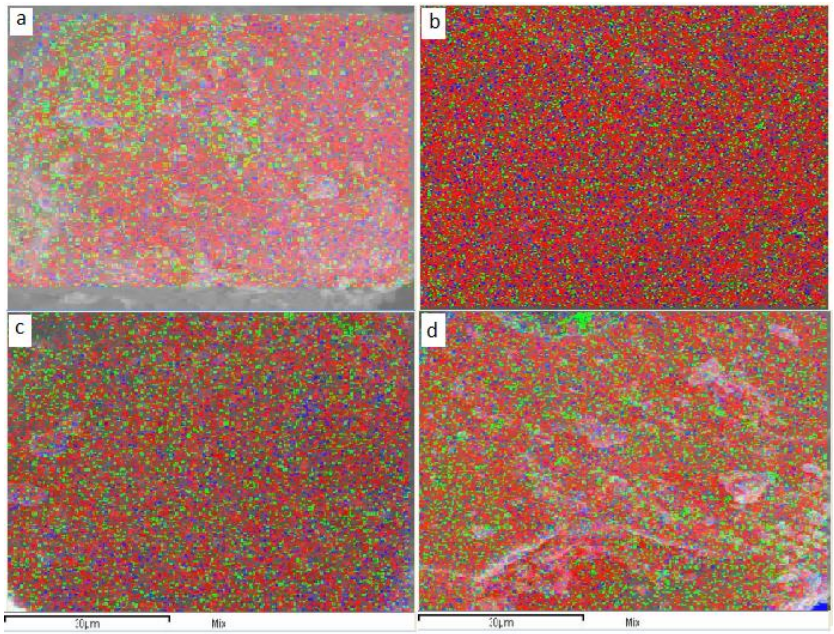

Fig. 5 : Elemental mapping images of a) MWCNTs/ Co-TiO_2 (3.03), b) MWCNTs/ Co-TiO_2 (3.13), c) MWCNTs/ Co-TiO_2 (3.52) and d) MWCNTs/ Co-TiO_2 (4.14).

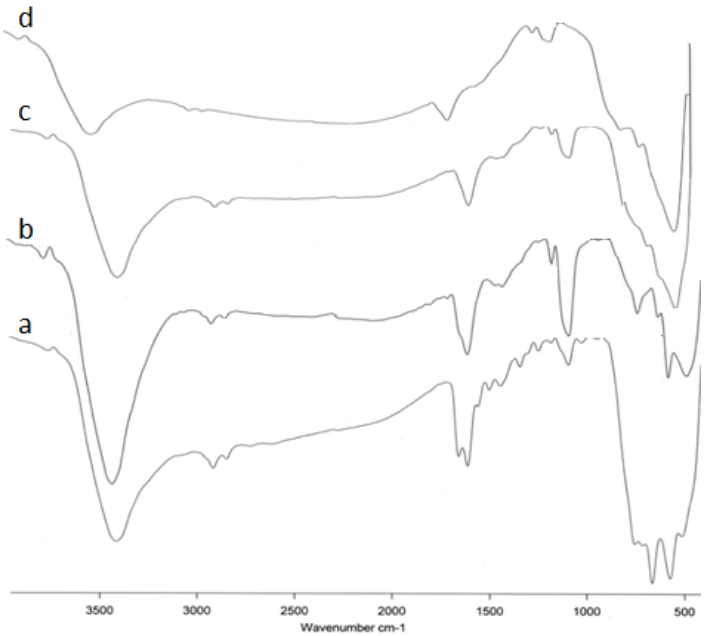

Fig. 6: FTIR spectra of of a) MWCNTs/ Co-TiO_2 (3.03), b) MWCNTs/ Co-TiO_2 (3.13), c) MWCNTs/ Co-TiO_2 (3.52) and d) MWCNTs/ Co-TiO_2 (4.14).

The abundant hydroxyl groups adsorbed on the surface of the catalyst could facilitate the formation of hydroxyl radicals which could optimize the degradation process of the adsorbed 2,4-DCP on the surface [46]. Thirdly, because of presence MWCNTs, the surface area of MWCNTs/Co-TiO_2 samples were slightly larger than that of pure TiO_2 which might favor the adsorption of 2,4-DCP and provide more possibly accessible active sites. Also, there is a synergetic effect between MWCNTs and TiO_2 and MWCNTs acting as a photosensitizer. MWCNTs can trap the photo-induced electrons and form superoxide radical ion and/or hydroxyl radical on the surface of TiO_2, which are responsible

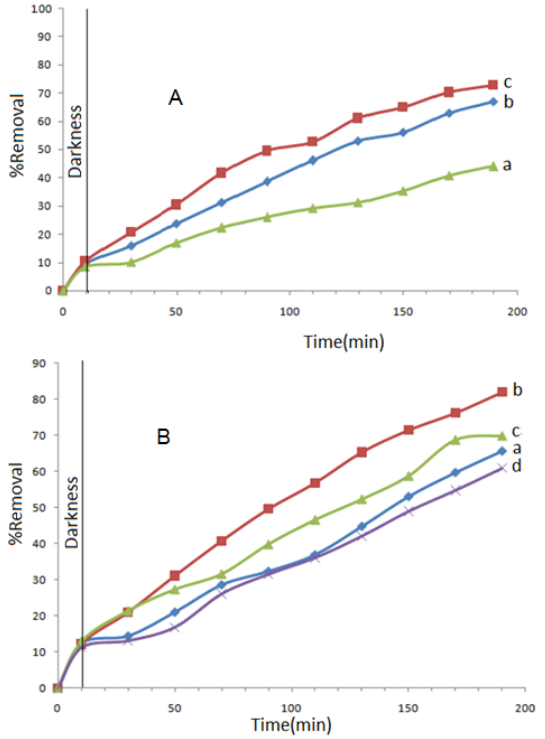

Fig. 7: Photocatalytic degradation of 2,4-DCP over A: (a) TiO_2, b) Co-TiO_2 and c) MWCNTs/TiO_2, B: a) MWCNTs/ Co-TiO_2 (3.03), b) MWCNTs/ Co-TiO_2 (3.13), c) MWCNTs/ Co-TiO_2 (3.52) and d) MWCNTs/ Co-TiO_2 (4.14) (2,4-DCP Conc. 40 mg/L, 10 mg catalyst, 100 mL 2,4-DCP, visible light, irradiation time: 180 min).

for the degradation of the organic compound. Due to the introduction of the MWCNTs, an increase of surface charge on TiO_2 in the hybrid catalysts can be suggested. The surface charge may lead to modifications of the fundamental process of electron/hole pair formation while applying visible irradiation [47]. Consequently, it may be the unique interaction between TiO_2 and the MWCNTs that endows the ternary nanocomposite with a higher catalytic activity in the photocatalytic removal of MO compares to pure TiO_2.

Also from Table 4, while Co dopant content increased from 3.03 wt.% to 3.13 wt.%, the dominant Co^{2+} captured electrons which then moved to the absorbed O_2 to reach a higher photocatalytic reaction. As the literature reported [48], with the substitution for $Ti^{4+}$by Co^{2+}in crystal structure of TiO_2, the catalyst can introduce a new impurity level to the conduction band of TiO_2 and the electrons can be promoted from the valence band to these impurity levels, resulting in a narrowing of the band gap. This fact indicates that there are more photogenerated electrons and holes which can be introduced to participate in the photocatalytic

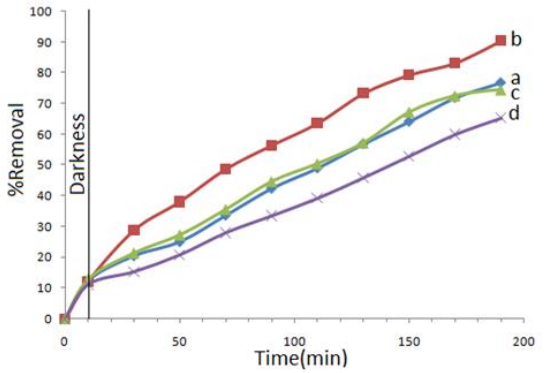

Fig. 8: Photocatalytic removal of 2,4-DCP over a) MWCNTs/ Co-TiO_2 (3.03), b) MWCNTs/ Co-TiO_2 (3.13), c) MWCNTs/ Co-TiO_2 (3.52) and d) MWCNTs/ Co-TiO_2 (4.14) (2,4-DCP Conc. 40 mg/L, 10 mg catalyst, 100 mL 2,4-DCP, visible light, irradiation time: 180 min and H_2O_2 conc. 0.01M).

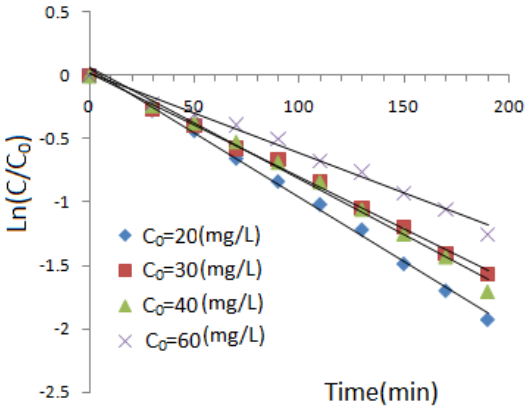

Fig. 9: Effect of initial concentration on the degradation of 2,4-DCP. Irradiation. source: visible lamp, 100mL 2,4-DCP, 10mg catalyst

reactions [49]. However, recombination of photogenerated electrons and holes is one of the most significant factors that deteriorate the photoactivity of the TiO_2 catalyst. Any factor that suppresses the electron-hole recombination will, therefore, enhance the photocatalytic activity[50,51]. In general, if the size of doping metal ion is very similar toTi^{4+}, it is very likely that metal ion enters into the interstitial site of the TiO_2 crystal. The doping metal ion located mainly on the shallow surface of TiO_2 can induce defects. The defects can become the centers of shallow electrons or holes traps, which would efficiently improve separation of an electron-hole pair. Hence the photocatalyst will have a high photocatalytic activity [52]. The radius of Co^{2+}(0.074 nm) is slightly bigger than Ti^{4+}(0.068 nm) [52]. When calcination was performed at high-temperature

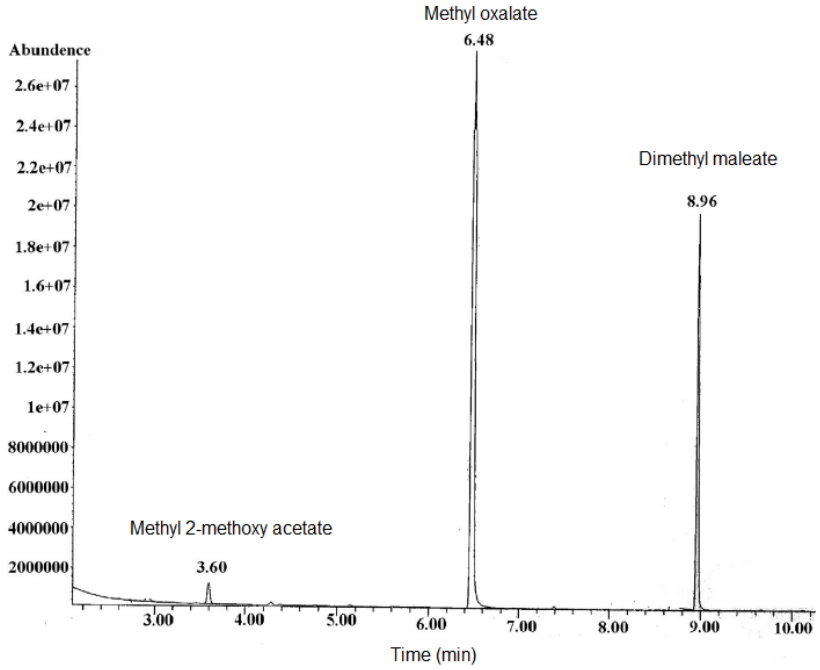

Fig. 10: GC chromatogram of the final products of the photocatalytic degradation of 2,4-DCP by MWCNTs/Co-TiO_2 (3.13).

Co^{2+}ions may enter the interstitial site of TiO_2 crystal and can create crystal defect. In this present work, FT-IR spectra revealed that there were Co–O bonds in the TiO_2/Co nanoparticles. The formation of the Co–O hindered the recombination of photogenerated electrons and holes, so the cobalt doping increased the photocatalytic activity of naked TiO_2. According to Fig. 7 and Table 4, 3.13 wt% was the optimal doping content. When the doping ratio is 3.52 or 4.14 wt%, the degradation rate became slower. This is because, at a low doping level of metal, photogenerated holes and electrons are well separated, increasing the efficiency of the photocatalyst. However, at high doping level, there is a considerable chance for multiple trapping which will reduce the efficiency of the catalyst. Moreover, the detrimental activity at high cobalt loading may be attributed to the blockage of many TiO_2 active sites due to the large amounts [40].

The activity of the samples for degradation of 2,4-DCP may even be better by addition of hydrogen peroxide to the reactor (Fig. 8). Almost 82% of 2,4-DCP is removed within 180 min in the presence of MWCNTs/Co-TiO_2 (3.13), when there is no H_2O_2 added. In the presence of H_2O_2, more hydroxyl radicals are produced compared to the conditions without using H_2O_2 and we obtained 91% removal for 2,4-DCP. Hydroxyl radicals may be generated by direct photolysis of hydrogen peroxide [53,54], or by reaction of hydrogen peroxide with superoxide radical [55, 56]. Since in our study a source of visible light is employed, it is unlikely that direct photolysis of hydrogen peroxide is significant. Basically, wavelengths shorter than 300 nm provide enough energy for photocleavage of the H_2O_2 molecules. This can be explained according to the below reaction:

$$H_2O_2 + O_2^{-*} \rightarrow OH^* + OH^- + O_2 \quad (2)$$

The faster hydroxyl radical formation is associated with the higher degradation rate. This photocatalyst did not exhibit any photoactivity in the dark, neither in the absence nor in the presence of H_2O_2, suggesting that it is necessary to photoexcite both TiO_2 and the cobalt in order to a obtain substantial improvement of the degradation of 2,4-DCP.

The kinetic of 2,4-DCP degradation

The photocatalytic degradation of 2,4-DCP is a first-order reaction and its kinetics may be expressed as $\ln(C/C_0) = -k_{obs}t$ (Fig. 9). In this equation k_{obs} (min^{-1}) is the apparent rate constant, C_0 and C are the initial concentration and concentration at reaction time t of 2,4-DCP, respectively. The k_{obs} are found from the slopes of the straight lines obtained by plotting $\ln(C/C_0)$ versus irradiation time (Fig. 9). The reaction rates, rate constants and half-lifes

Table 5: The rate, rate constant (k_{obs}) and half-time ($t_{1/2}$) for various concentrations of 2,4-DCP.after 180 min.

Concentration (mg/L)	R^2	Initial reaction rate (mg/L.(min^{-1}))	k_{obs}(min^{-1})	$t_{1/2}$ (min)
20	0.9964	0.202	0.0101	68.61
30	0.9958	0.264	0.0088	78.75
40	0.9916	0.328	0.0082	84.51
60	0.9906	0.378	0.0063	110.00

R^2 shows correlation coefficient for fit experimental data (Fig. 9)

($t_{1/2}$) at various initial concentrations of 2,4-DCP are given in Table 5. The results summarized in Table 5 show that the reaction rate of degradation of 2,4-DCP is faster at higher initial concentration. However, the rate constants decrease to some extent when the initial concentration increases.

Identification of intermediate products

The intermediate species formed during photocatalytic degradation of 2,4- DCP, were identified by GC–MS technique. The major reaction intermediates identified in an aliquot withdrawn after 200 min following a degradation condition specified as in Fig. 7. Presence of these intermediates (Fig. 10) supports our proposed mechanism which is based on OH radicals. The hydroxyl radicals attack 2,4-DCP converting it to chlorocatechol and then to chlorobenzoquinone. Subsequently, hydroxyl groups would break the aromatic rings of chlorobenzo-quinone transferring them into simple acids like oxalic acid, acetic acid, etc. as the final products [57,58]. In addition to identifying the organic intermediates, chloride ions were also detected and identified as one of the final products of the photocatalytic removal. The amount of Cl^- in the reaction media at the end of the photocatalytic experiment almost equals the amount of chlorine present in 2,4-DCP indicating essentially complete degradation.

Photocatalyst reuse

The effectiveness of photocatalyst reuse was examined for degradation of 2,4-DCP during a four cycles experiment. Each experiment was carried out under identical conditions. 100mL 2,4-DCP with an initial concentration of 40 mg/L, 10mg MWCNTs/Co-TiO_2 (3.13) and 180 min irradiation time under visible light were used. After each experiment, the solution residue from the photocatalytic degradation was filtered, washed and the solid was dried. The dried catalyst samples were used again for the degradation of 2,4-DCP, employing similar experimental conditions. Recycling experiments showed, no obvious decrease of the photocatalytic removal efficiency (from 82% to 78%) was observed after four cycles and indicating that our MWCNTs/Co-TiO_2 (3.13) is renewable for environmental applications. Possibly deactivation of the part of the photocatalyst surface, due to permanent adsorption of intermediate species, might be involved in the reduction of its activity.

CONCLUSIONS

In summary, ternary MWCNTs /Co-TiO_2 nanocomposites were successfully prepared by the modified sol-gel process and characterized by a different analysis. It was found that the ternary MWCNTs /Co-TiO_2 nanocomposites presented enhanced photocatalytic degradation of 2,4-dichlorophenol (2,4-DCP) and exhibited expansion in spectral response range shifted to the visible region. This was probably due to the affiliation of special properties by MWCNTs and Co dopant. The presence of MWCNTs could create many active sites and increase surface area while Co doping promoted the separation of photogenerated carriers. Furthermore, the major problem of TiO_2 photocatalyst was reduced by narrowing their band gap by the Co dopant. Therefore, adding a suitable amount of MWCNTs and Co into the TiO_2 lead to a great improvement in the photocatalytic degradation of 2,4-DCP and this new photocatalyst showed remarkable activity in the visible light region. The reactions follow a pseudo-first-order kinetics and the observed rate constant values change with 2,4-DCP concentrations. Oxalic acid and maleic acid were the major intermediate species at the final stage of the degradation process as identified by gas chromatography-mass spectrometry (GC–MS) technique.

ACKNOWLEDGEMENTS

The authors wish to acknowledge the financial support of the University of Tehran for supporting this research.

CONFLICT OF INTEREST

The authors declare that there is no conflict of interests regarding the publication of this manuscript.

REFERENCES

1. Anandan S. Photocatalytic effects of titania supported nanoporous MCM-41 on degradation of methyl orange in the presence of electron acceptors. Dyes and Pigments. 2008;76(2):535-41.
2. Lam S-M, Sin J-C, Mohamed AR. Parameter effect on photocatalytic degradation of phenol using TiO2-P25/ activated carbon (AC). Korean Journal of Chemical Engineering. 2010;27(4):1109-16.
3. Ahlborg UG, Thunberg TM, Spencer HC. Chlorinated Phenols: Occurrence, Toxicity, Metabolism, And Environmental Impact. CRC Critical Reviews in Toxicology. 1980;7(1):1-35.
4. Lee H-C, In J-H, Kim J-H, Hwang K-Y, Lee C-H. Kinetic analysis for decomposition of 2,4-dichlorophenol by supercritical water oxidation. Korean Journal of Chemical Engineering. 2005;22(6):882-8.
5. Dionysiou DD, Khodadoust AP, Kern AM, Suidan MT, Baudin I, Laîné J-M. Continuous-mode photocatalytic degradation of chlorinated phenols and pesticides in water using a bench-scale TiO2 rotating disk reactor. Applied Catalysis B: Environmental. 2000;24(3):139-55.
6. Arnoldsson K, Andersson PL, Haglund P. Formation of Environmentally Relevant Brominated Dioxins from 2,4,6,-Tribromophenol via Bromoperoxidase-Catalyzed Dimerization. Environmental Science & Technology. 2012;46(13):7239-44.
7. Bandara J, Mielczarski JA, Lopez A, Kiwi J. 2. Sensitized degradation of chlorophenols on iron oxides induced by visible light: Comparison with titanium oxide. Applied Catalysis B: Environmental. 2001;34(4):321-33.
8. White JL, Baruch MF, Pander JE, Hu Y, Fortmeyer IC, Park JE, et al. Light-Driven Heterogeneous Reduction of Carbon Dioxide: Photocatalysts and Photoelectrodes. Chemical Reviews. 2015;115(23):12888-935.
9. Liu J, Bai H, Wang Y, Liu Z, Zhang X, Sun DD. Self-Assembling TiO2 Nanorods on Large Graphene Oxide Sheets at a Two-Phase Interface and Their Anti-Recombination in Photocatalytic Applications. Advanced Functional Materials. 2010;20(23):4175-81.
10. Ashford DL, Gish MK, Vannucci AK, Brennaman MK, Templeton JL, Papanikolas JM, et al. Molecular Chromophore–Catalyst Assemblies for Solar Fuel Applications. Chemical Reviews. 2015;115(23):13006-49.
11. Ioannidou E, Ioannidi A, Frontistis Z, Antonopoulou M, Tselios C, Tsikritzis D, et al. Correlating the properties of hydrogenated titania to reaction kinetics and mechanism for the photocatalytic degradation of bisphenol A under solar irradiation. Applied Catalysis B: Environmental. 2016;188(Supplement C):65-76.
12. Wang H, Wang H-L, Jiang W-F, Li Z-Q. Photocatalytic degradation of 2,4-dinitrophenol (DNP) by multi-walled carbon nanotubes (MWCNTs)/TiO2 composite in aqueous solution under solar irradiation. Water Research. 2009;43(1):204-10.
13. Sarteep Z, Ebrahimian Pirbazari A, Aroon MA. Silver Doped TiO2 Nanoparticles: Preparation, Characterization and Efficient Degradation of 2,4-dichlorophenol Under Visible Light. Journal of Water and Environmental Nanotechnology. 2016;1(2):135-44.
14. Devi LG, Kottam N, Murthy BN, Kumar SG. Enhanced photocatalytic activity of transition metal ions Mn2+, Ni2+ and Zn2+ doped polycrystalline titania for the degradation of Aniline Blue under UV/solar light. Journal of Molecular Catalysis A: Chemical. 2010;328(1):44-52.
15. Gurkan YY, Kasapbasi E, Cinar Z. Enhanced solar photocatalytic activity of TiO2 by selenium(IV) ion-doping: Characterization and DFT modeling of the surface. Chemical Engineering Journal. 2013;214(Supplement C):34-44.
16. Zou X-X, Li G-D, Guo M-Y, Li X-H, Liu D-P, Su J, et al. Heterometal Alkoxides as Precursors for the Preparation of Porous Fe– and Mn–TiO2 Photocatalysts with High Efficiencies. Chemistry – A European Journal. 2008;14(35):11123-31.
17. Feng H, Zhang M-H, Yu LE. Hydrothermal synthesis and photocatalytic performance of metal-ions doped TiO2. Applied Catalysis A: General. 2012;413(Supplement C):238-44.
18. Van Nghia N, Ngoc Khoa Truong N, Phi Hung N. Hydrothermal synthesis of Fe-doped TiO 2 nanostructure photocatalyst. Advances in Natural Sciences: Nanoscience and Nanotechnology. 2011;2(3):035014-8.
19. Pirbazari AE, Monazzam P, Kisomi BF. Co/TiO2 Nanoparticles: Preparation, Characterization and Its Application for Photocatalytic Degradation of Methylene Blue. Desalination and Water Treatment. 2017;63:283-92.
20. Iwasaki M, Hara M, Kawada H, Tada H, Ito S. Cobalt Ion-Doped TiO2 Photocatalyst Response to Visible Light. Journal of Colloid and Interface Science. 2000;224(1):202-4.
21. Liu SX, Chen XY, Chen X. A TiO2/AC composite photocatalyst with high activity and easy separation prepared by a hydrothermal method. Journal of Hazardous Materials. 2007;143(1):257-63.
22. Sakthivel S, Kisch H. Daylight Photocatalysis by Carbon-Modified Titanium Dioxide. Angewandte Chemie International Edition. 2003;42(40):4908-11.
23. Zhang L-W, Fu H-B, Zhu Y-F. Efficient TiO2 Photocatalysts from Surface Hybridization of TiO2 Particles with Graphite-like Carbon. Advanced Functional Materials. 2008;18(15):2180-9.
24. Iijima S. Helical microtubules of graphitic carbon. Nature. 1991;354(6348):56-8.
25. Yu M-F, Files BS, Arepalli S, Ruoff RS. Tensile loading of ropes of single wall carbon nanotubes and their mechanical properties. Physical review letters. 2000;84(24):5552-3.
26. Cha SI, Kim KT, Lee KH, Mo CB, Jeong YJ, Hong SH. Mechanical and electrical properties of cross-linked carbon nanotubes. Carbon. 2008;46(3):482-8.
27. Serp P, Corrias M, Kalck P. Carbon nanotubes and nanofibers in catalysis. Applied Catalysis A: General. 2003;253(2):337-58.
28. Wang W, Serp P, Kalck P, Faria JL. Photocatalytic degradation of phenol on MWNT and titania composite catalysts prepared by a modified sol–gel method. Applied Catalysis B: Environmental. 2005;56(4):305-12.
29. Lee TY, Alegaonkar PS, Yoo J-B. Fabrication of dye sensitized solar cell using TiO2 coated carbon nanotubes. Thin Solid

Films. 2007;515(12):5131-5.

30. Yao Y, Li G, Ciston S, Lueptow RM, Gray KA. Photoreactive TiO2/Carbon Nanotube Composites: Synthesis and Reactivity. Environmental Science & Technology. 2008;42(13):4952-7.
31. Baiju KV, Shajesh P, Wunderlich W, Mukundan P, Kumar SR, Warrier KGK. Effect of tantalum addition on anatase phase stability and photoactivity of aqueous sol–gel derived mesoporous titania. Journal of Molecular Catalysis A: Chemical. 2007;276(1):41-6.
32. Ahmmad B, Kusumoto Y, Somekawa S, Ikeda M. Carbon nanotubes synergistically enhance photocatalytic activity of TiO2. Catalysis Communications. 2008;9(6):1410-3.
33. Wang W, Serp P, Kalck P, Faria JL. Visible light photodegradation of phenol on MWNT-TiO2 composite catalysts prepared by a modified sol–gel method. Journal of Molecular Catalysis A: Chemical. 2005;235(1):194-9.
34. Jiang P, Xiang W, Kuang J, Liu W, Cao W. Effect of cobalt doping on the electronic, optical and photocatalytic properties of TiO2. Solid State Sciences. 2015;46(Supplement C):27-32.
35. Chen Q, Ji F, Liu T, Yan P, Guan W, Xu X. Synergistic effect of bifunctional Co–TiO2 catalyst on degradation of Rhodamine B: Fenton-photo hybrid process. Chemical Engineering Journal. 2013;229(Supplement C):57-65.
36. Preethi T, Abarna B, Vidhya KN, Rajarajeswari GR. Sol–gel derived cobalt doped nano-titania photocatalytic system for solar light induced degradation of crystal violet. Ceramics International. 2014;40(8, Part B):13159-67.
37. Kaushik A, Dalela B, Kumar S, Alvi PA, Dalela S. Role of Co doping on structural, optical and magnetic properties of TiO2. Journal of Alloys and Compounds. 2013;552(Supplement C):274-8.
38. Fan C, Xue P, Sun Y. Preparation of Nano-TiO2 Doped with Cerium and Its Photocatalytic Activity. Journal of Rare Earths. 2006;24(3):309-13.
39. Khan M, Cao W. Cationic (V, Y)-codoped TiO2 with enhanced visible light induced photocatalytic activity: A combined experimental and theoretical study. Journal of Applied Physics. 2013;114(18):183514.
40. Vijayan P, Mahendiran C, Suresh C, Shanthi K. Photocatalytic activity of iron doped nanocrystalline titania for the oxidative degradation of 2,4,6-trichlorophenol. Catalysis Today. 2009;141(1):220-4.
41. Silva CG, Faria JL. Photocatalytic oxidation of benzene derivatives in aqueous suspensions: Synergic effect induced by the introduction of carbon nanotubes in a TiO2 matrix. Applied Catalysis B: Environmental. 2010;101(1):81-9.
42. Zhang K, Zhang FJ, Chen ML, Oh WC. Comparison of catalytic activities for photocatalytic and sonocatalytic degradation of methylene blue in present of anatase TiO2–CNT catalysts. Ultrasonics Sonochemistry. 2011;18(3):765-72.
43. Wang Y, Huang Y, Ho W, Zhang L, Zou Z, Lee S. Biomolecule-controlled hydrothermal synthesis of C–N–S-tridoped TiO2 nanocrystalline photocatalysts for NO removal under simulated solar light irradiation. Journal of Hazardous Materials. 2009;169(1):77-87.
44. Bae E, Choi W. Highly Enhanced Photoreductive Degradation of Perchlorinated Compounds on Dye-Sensitized Metal/TiO2 under Visible Light. Environmental Science & Technology. 2003;37(1):147-52.
45. Guo Q, Guo X, Tian Q. Optionally ultra-fast synthesis of CoO/Co3O4 particles using CoCl2 solution via a versatile spray roasting method. Advanced Powder Technology. 2010;21(5):529-33.
46. Yang Q, Deng Y, Hu W. Preparation of alumina/carbon nanotubes composites by chemical precipitation. Ceramics International. 2009;35(3):1305-10.
47. Wang W, Serp P, Kalck P, Faria JL. Visible light photodegradation of phenol on MWNT-TiO2 composite catalysts prepared by a modified sol–gel method. Journal of Molecular Catalysis A: Chemical. 2005;235(1):194-9.
48. Yang J, Cui S, Qiao J-q, Lian H-z. The photocatalytic dehalogenation of chlorophenols and bromophenols by cobalt doped nano TiO2. Journal of Molecular Catalysis A: Chemical. 2014;395(Supplement C):42-51.
49. Li C-J, Wang J-N, Wang B, Gong JR, Lin Z. A novel magnetically separable TiO2/CoFe2O4 nanofiber with high photocatalytic activity under UV–vis light. Materials Research Bulletin. 2012;47(2):333-7.
50. Sakthivel S, Shankar MV, Palanichamy M, Arabindoo B, Bahnemann DW, Murugesan V. Enhancement of photocatalytic activity by metal deposition: characterisation and photonic efficiency of Pt, Au and Pd deposited on TiO2 catalyst. Water Research. 2004;38(13):3001-8.
51. Nagaveni K, Hegde MS, Madras G. Structure and Photocatalytic Activity of Ti1-xMxO2±δ (M = W, V, Ce, Zr, Fe, and Cu) Synthesized by Solution Combustion Method. The Journal of Physical Chemistry B. 2004;108(52):20204-12.
52. Chand R, Obuchi E, Katoh K, Luitel HN, Nakano K. Effect of transition metal doping under reducing calcination atmosphere on photocatalytic property of TiO2 immobilized on SiO2 beads. Journal of Environmental Sciences. 2013;25(7):1419-23.
53. Peyton GR, Glaze WH. Destruction of pollutants in water with ozone in combination with ultraviolet radiation. 3. Photolysis of aqueous ozone. Environmental Science & Technology. 1988;22(7):761-7.
54. Ollis DF, Pelizzetti E, Serpone N. Photocatalyzed destruction of water contaminants. Environmental Science & Technology. 1991;25(9):1522-9.
55. Poulios I, Micropoulou E, Panou R, Kostopoulou E. Photooxidation of eosin Y in the presence of semiconducting oxides. Applied Catalysis B: Environmental. 2003;41(4):345-55.
56. Cornish BJPA, Lawton LA, Robertson PKJ. Hydrogen peroxide enhanced photocatalytic oxidation of microcystin-LR using titanium dioxide. Applied Catalysis B: Environmental. 2000;25(1):59-67.
57. Shibata T, Irie H, Tryk DA, Hashimoto K. Effect of Residual Stress on the Photochemical Properties of TiO2 Thin Films. The Journal of Physical Chemistry C. 2009;113(29):12811-7.
58. Chaliha S, Bhattacharyya KG. Fe(III)-, Co(II)- and Ni(II)-impregnated MCM41 for wet oxidative destruction of 2,4-dichlorophenol in water. Catalysis Today. 2009;141(1):225-33.